ISIT'2013 1569719219

Fractionally Spaced Equalization for Broadband Amplify-and-forward Cooperative Systems

Mohammad R. Heidarpour[1] , Murat Uysal[2,1], and Mohamed Oussama Damen[1]

[1]Department of Electrical and Computer Engineering, University of Waterloo, Waterloo, Ontario, Canada
[2] Department of Electrical and Electronics Engineering, Özyeğin University, Istanbul, Turkey

***Abstract*—In this paper, we revisit the concept of fractionally spaced equalization (FSE) for broadband single-carrier amplify-and-forward (AaF) cooperative systems. Particularly, we investigate fractionally spaced frequency domain equalization (FS-FDE) for cooperative multi-relay systems. Our motivation stems from the elegant properties reported for the FSE in the point-to-point communication systems (i.e., its robustness to sampling phases and potential in achieving the optimum performance) and the scalability of the FDEs. In particular, we propose a $T_S/2$-spaced equalizer that transforms the temporal sample sequence of the received signal to the frequency domain, applies linear/decision-feedback equalization, and returns the resulting signal back to the time domain for detection. The vital importance of using FS-FDE method in cooperative systems is disclosed in practical scenarios where the transmitted signals have non-zero roll-off components and sampling phase error may occur in relay(s) and destination terminals. Our results demonstrate that, under specific channel realizations and sampling errors, the cooperative systems with symbol spaced FDE (SS-FDE) fail to harvest the available cooperative diversity and the performance approaches to that of no relay scenario. On the other hand, the performance of cooperative system with FS-FDE method becomes independent of sampling phase errors and full benefit of cooperation is retained.**

***Keywords*—Cooperative diversity, Fractionally spaced equalization**

I. Introduction

Cooperative communication exploits the broadcasting nature of wireless transmission and creates a virtual antenna array among the source and some partner nodes [1]. These partner nodes that are willing to share their resources with the source and the destination nodes are commonly referred to as relays. Relays operate under different modes including decode-and-forward (DaF) and amplify-and-forward (AaF) relaying. In DaF relaying, the relay attempts to decode its received signal and, if successful, then participates in the relaying phase by transmitting the re-encoded version of the information towards the destination. On the other hand, in AaF relaying, the relay node simply scales the received signal to avoid power budget violation and then transmits the resulting signal to the destination.

The conventional technique to combat the inter-symbol-interference (ISI) impairment in the broadband single-carrier wireless systems is channel equalization [2, 3]. One way to categorize equalization techniques is based on the sampling rates. In the symbol-spaced equalizers (SSEs), the received signal is sampled at the symbol (or baud) rate before applying to the equalization filter. As a result, in practical systems using pulse-shaping filters with non-zero roll-off factor, the equalization filter operates on an aliased spectrum of the received signal rendering performance acutely sensitive to the receiver sampling phase [4, 5]. The sampling phase sensitivity of SSEs can be avoided by the implementation of fractionally spaced equalizers (FSEs) in which the received signal is sampled at least as fast as the Nyquist rate [4, 6]. In [4], it is shown that unconstraint-length FSE achieves the optimum (in the minimum-mean-square error [MMSE] sense) performance of the linear receivers. On the other hand, different equalization methods are also classified based on their operation in time or frequency domain. In the high data-rate communication, specifically in highly dispersive channels, the complexity demand of the time-domain equalization (TDE) becomes prohibitively high, whereas, the frequency domain equalization (FDE) exhibits a low complexity growth by increasing the data rate and/or the length of the underlying channel impulse response [7].

Although the theory of equalization is enriched for the point-to-point communications including multiple-input multiple-output (MIMO) systems [7, 8], it is an under-explored concept for the case of cooperative systems and limited to a few publications (see [9–12] and references therein). One of the earliest works on this topic is [9], where Mheidat et. al. proposed some symbol spaced FDE (SS-FDE) techniques for several cooperative systems. Based on maximizing signal-to-noise ratio (SNR), the design of symbol spaced TDE (SS-TDE) in the relays for cooperative beamforming transmission is proposed in [10], and pursued by also considering SS-TDE filtering at the destination terminal in [11]. Considering the use of SS-FDE filters instead of SS-TDE ones, the design of cooperative beamforming systems is also revisited in [12].

To the best of our knowledge, FSE has not yet been studied in the context of cooperative systems. In this paper, we investigate fractionally spaced FDE (FS-FDE) technique for a cooperative multi-relay system. Our motivation stems from the elegant properties reported for the FSEs in the point-to-point communication systems (i.e., its robustness to sampling phases and potential in achieving the optimum performance) and the scalability of the FDEs. In particular, we propose a $T_S/2$-spaced equalizer (used often in many applications, even in cases where a larger tap spacing is possible [2]) that transforms the temporal sample sequence of the received signal to the frequency domain, applies MMSE linear/decision-feedback equalization, and returns the resulting signal back to the time domain for detection. The vital importance of using FSE method in cooperative systems is disclosed in practical scenarios where the transmitted signals have non-zero roll-off components and sampling phase error may occur in relay(s) and destination terminals. Analytical and numerical results are reported to compare the performance of FS-FDE and SS-FDE based cooperative systems. Specifically, it is observed that, under specific channel realizations and sampling errors, the cooperative systems with SS-FDE fail to harvest the available cooperative diversity and the performance approaches to that of no relay scenario. On the other hand, the performance of cooperative systems with FS-FDE method becomes independent of sampling phase errors and full benefit of cooperation is retained.

The rest of the paper is organized as follows. In Section II, we introduce the system model. In Section III, we present the

This work is supported, in part, by the TUBITAK Research Grant (110E092) and, in part, by TUBA GEBIP.

derivation of the FS-FDEs and SS-FDEs. In Section IV, we present simulation results. Finally, we conclude in Section V.

Notation: Bold upper-case letters denote matrices and bold lower-case letters denote column vectors. $(.)^T$ and $(.)^*$ are the transpose and conjugate transpose operations, respectively. $*$ is the linear convolution operator. $\otimes$ denotes Kronecker product. $< . >_N$ is the modulo N operation. $[k]_N = k$ if $k \leq N$, and $[k]_N = k - 2N$ if $k > N$. $\delta(n)$ is the Kronecker delta function. $\|\mathbf{x}\|$ denotes the Euclidean norm of the vector $\mathbf{x}$. E[.] denotes expectation. $\mathrm{trace}(\mathbf{X})$ denotes the trace of matrix $\mathbf{X}$. $\mathrm{diag}\{\mathbf{x}\}$ stands for a diagonal matrix with elements of vector $\mathbf{x}$ on its diagonal. $[\mathbf{X}|\mathbf{Y}]$ denotes a matrix obtained by concatenation of matrices $\mathbf{X}$ and $\mathbf{Y}$. $\mathbf{I}_K$ denotes the identity matrix of size K. $\mathbf{0}_{M\times N}$ and $\mathbf{1}_{M\times N}$ denote $M \times N$ all-zero and all-one matrices, respectively. $\mathbf{Q}_N = [q_{n,k}]$ is the N-point discrete Fourier transform (DFT) matrix $(n, k = 0, 1, \ldots, N-1)$ with $q_{n,k} = \frac{1}{\sqrt{N}} W_N^{kn}$ and $W_N \triangleq \exp(-j\frac{2\pi}{N})$.

II. System Model

In the cooperative system under consideration, the source node S transmits information to the destination node D through the assistance of M relay nodes $R_1, \ldots, R_M$(See Fig. 1). We consider an aggregate channel model which consists of both long-term path loss and short-term fading effects. Normalizing the path-loss in the source-to-destination link to be unity, the relative gain in the A→B link[1] is defined by G_{AB}. The short term variations of the underlying channels are also modelled as frequency-selective Rayleigh fading. In particular, the channel impulse response of A→B link is represented by $h_{\mathrm{AB}}(t) = \sum_{n=0}^{L_{\mathrm{AB}}-1} \mathbf{h}_{\mathrm{AB}}(n)\delta(t-\boldsymbol{\tau}_{\mathrm{AB}}(n))$ where L_{AB} denotes the number of resolvable paths and the vector $\boldsymbol{\tau}_{\mathrm{AB}}$ includes the delays associated with different paths. The entries of random vector $\mathbf{h}_{\mathrm{AB}}$ are independent identically distributed (i.i.d.) zero-mean complex Gaussian random variables with variances $1/L_{\mathrm{AB}}$. It is also assumed that the temporal support of $h_{\mathrm{AB}}(t)$ is less than or equal to l_{AB} symbol intervals, and the coherence time of $h_{\mathrm{AB}}(t)$ is more than that of required for the transmission of one block of data.

In this paper, we consider opportunistic cooperation with AaF relaying [1]. The block diagrams of the source, relay and destination terminals are illustrated in Fig. 2. We assume the cyclic prefix single- carrier (CPSC) transmission. At the source terminal (see Fig. 2a), a stream of $N\log\Theta$ bits is parsed into N consecutive tuples of $\log\Theta$ bits. Each tuple is mapped (using Gray coding) into a complex channel symbol belonging to a Θ-point linear-modulation constellation (such as PSK or QAM) with unit average power. The resulting sequence of symbols, denoted by $\mathbf{a} = [a_0, \ldots, a_{N-1}]^T$, is appended by a cyclic prefix (CP) with length N_1, and fed to the transmitter filter at a rate of $1/T_S$ where T_S seconds is the signalling interval. The impulse response of the filter is given by the unit-energy root-raised-cosine function $g(t)$ with the temporal support in the range of $[0, N_{RRC}T_S]$ and bandwidth $B_{RRC} = \frac{1}{2T_S}(1+\beta)$ where $0 \leq \beta \leq 1$ is the roll-off factor. After power amplification, the baseband signal transmitted by the source is given by

$$x_{\mathrm{S}}(t) = \sqrt{P_0} \sum_{n=-N_1}^{N-1} \mathbf{a}(< n >_N) g(t - nT_S) \tag{1}$$

where P_0 is the average source power per symbol and can be written as $P_0 = K_0 P_T$ $(0 \leq K_0 \leq 1)$. Here, P_T denotes the average total power budget (i.e., total power of source and relay nodes) for transmitting one symbol. Accordingly,

[1] A→B signifies the link between nodes A and B.

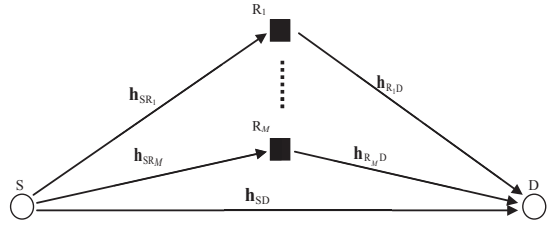

Fig. 1: The general configuration of the cooperative systems under consideration

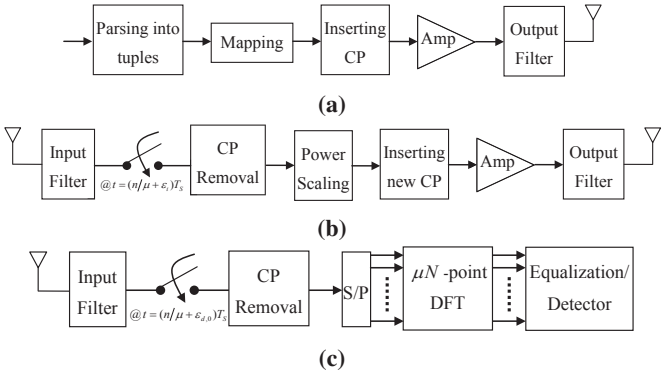

Fig. 2: Block diagram of (a) source, (b) relay, and (c) destination

the received signals at the mth relay and the destination are respectively, given by

$$r_{\mathrm{SR}_m}(t) = \sqrt{G_{\mathrm{SR}_m}P_0} \sum_{n=-N_1}^{N} \mathbf{a}(< n >_N) g(t - nT_S) * h_{\mathrm{SR}_m}(t) + n_{\mathrm{SR}_m}(t) \tag{2}$$

$$r_{\mathrm{SD}}(t) = \sqrt{P_0} \sum_{n=-N_1}^{N} \mathbf{a}(< n >_N) g(t - nT_S) * h_{\mathrm{SD}}(t) + n_{\mathrm{SD}}(t) \tag{3}$$

where $n_{\mathrm{SD}}(t)$ and $n_{\mathrm{SR}_m}(t)$ are the additive white complex Gaussian noises with zero mean and double sided power spectral density (PSD), N_0.

At the relay and destination (see Figs. 2b and 2c), the received signal is passed through the input filter with impulse response $p(t)$. For the case of SS-FDE, $p(t) = g^*(-t)$, and for the case of FS-FDE, $p(t)$ is an anti-aliasing low-pass filter given by $p(t) = \sqrt{T_S/2}\ \mathrm{sinc}(2t/T_S)$ [3].

Assume that $N_1 = \max(l_{\mathrm{SD}}, l_{\mathrm{SR}_1}, \ldots, l_{\mathrm{SR}_M}) + N_{RRC} + N_{sp,1}$ where $N_{sp,1}$ is the number of additional CP symbols inserted to the CPSC signal for the ease of symbol synchronization. The periodicity feature of the DFT allows us to represent the received signals at the destination and the mth relay as [6]

$$y_{\mathrm{SD}}(t) = \sqrt{\frac{P_0}{N}} \sum_{k=-N}^{N} \tilde{H}_{\mathrm{SD}}(k)\tilde{a}(k) e^{\frac{j2\pi kt}{NT_S}} + v_{\mathrm{SD}}(t) \tag{4}$$

$$y_{\mathrm{SR}_m}(t) = \sqrt{\frac{G_{\mathrm{SR}_m}P_0}{N}} \sum_{k=-N}^{N} \tilde{H}_{\mathrm{SR}_m}(k)\tilde{a}(k) e^{\frac{j2\pi kt}{NT_S}} + v_{\mathrm{SR}_m}(t) \tag{5}$$

for $-N_{sp,1}T_S \leq t \leq NT_S$ where $\tilde{a}(k) = \frac{1}{\sqrt{N}} \sum_{n=0}^{N-1} \mathbf{a}(n) W_N^{kn}$, $\tilde{H}_{\mathrm{SD}}(k) = \tilde{h}_{\mathrm{SD}}(k)\tilde{g}(k)\tilde{p}(k)$, $\tilde{H}_{\mathrm{SR}_m}(k) = \tilde{h}_{\mathrm{SR}_m}(k)\tilde{g}(k)\tilde{p}(k)$, $\tilde{g}(k) \triangleq \frac{\tilde{g}(\frac{k}{NT_S})}{\sqrt{T_S}}$, $\tilde{p}(k) \triangleq \frac{\tilde{p}(\frac{k}{NT_S})}{\sqrt{T_S}}$, $\tilde{h}_{\mathrm{SD}}(k) \triangleq \tilde{h}_{\mathrm{SD}}(\frac{k}{NT_S})$, $\tilde{h}_{\mathrm{SR}_m}(k) \triangleq \tilde{h}_{\mathrm{SR}_m}(\frac{k}{NT_S})$ with $\tilde{g}(f)$, $\tilde{p}(f)$, $\tilde{h}_{\mathrm{SD}}(f)$, $\tilde{h}_{\mathrm{SR}_m}(f)$ denoting the continuous Fourier transform of, respectively, $g(t)$, $p(t)$, $h_{\mathrm{SD}}(t)$, and $h_{\mathrm{SR}_m}(t)$. In (4) and (5), $v_{\mathrm{SD}}(t)$ and $v_{\mathrm{SR}_m}(t)$ are also coloured Gaussian noises with PSD

$S_0(f) = N_0|\tilde{p}(f)|^2$.

The received signals $y_{\mathrm{SD}}(t)$, and $y_{\mathrm{SR}_m}(t)$ are sampled at a rate of μ/T_S where $\mu = 1$ in the SS-FDE and $\mu = 2$ in the FS-FDE scheme. Therefore, from (4), and (5), we have

$$\mathbf{y}_{\mathrm{SD}}(n) = y_{\mathrm{SD}}(n\frac{T_S}{\mu} + \varepsilon_{d,0}T_S)$$
$$= \sqrt{\frac{P_0}{N}} \sum_{k=-N}^{N} \tilde{H}_{\mathrm{SD}}(k)\tilde{a}(k)W_N^{-k\varepsilon_{d,0}}W_{\mu N}^{-kn} + \mathbf{v}_{\mathrm{SD}}(n) \quad (6)$$

$$\mathbf{y}_{\mathrm{SR}_m}(n) = y_{\mathrm{SR}_m}(n\frac{T_S}{\mu} + \varepsilon_m T_S) = \sqrt{\frac{G_{\mathrm{SR}_m}P_0}{N}}$$
$$\times \sum_{k=-N}^{N} \tilde{H}_{\mathrm{SR}_m}(k)\tilde{a}(k)W_N^{-k\varepsilon_m}W_{\mu N}^{-kn} + \mathbf{v}_{\mathrm{SR}_m}(n) \quad (7)$$

for $n = 0, \ldots, \mu N - 1$, where $\mathbf{v}_{\mathrm{SD}}(n) = v_{\mathrm{SD}}(\frac{nT_S}{\mu} + \varepsilon_{d,0}T_S)$, $\mathbf{v}_{\mathrm{SR}_m}(n) = v_{\mathrm{SR}_m}(\frac{nT_S}{\mu} + \varepsilon_m T_S)$, $\varepsilon_{d,0}T_S$ is the sampling phase error in the destination, and $\varepsilon_m T_S$ is the sampling phase error in the mth relay ($-N_{sp,1} \le \varepsilon_{d,0}, \varepsilon_m \le 0$).

Assume that the ith relay is selected to transmit its signal. First, a CP with length $N_2 = \mu(l_{\mathrm{R}_i\mathrm{D}} + N_{RRC} + N_{sp,2})$ is inserted into the sampled sequence $\mathbf{y}_{\mathrm{SR}_i}$, and then the resulting signal with a rate of μ/T_S is applied to the pulse shaping filter followed by scaling and power amplification. Therefore, the baseband signal transmitted by the ith relay can be expressed as

$$x_{\mathrm{R}_i}(t) = \sqrt{\alpha_{\mathrm{R}_i}P_1} \sum_{n=-N_2}^{\mu N-1} \mathbf{y}_{\mathrm{SR}_i}(< n >_{\mu N})g(t - \frac{nT_S}{\mu}) \quad (8)$$

where α_{R_i} is the scaling factor to ensure that the average power consumed per symbol by the ith relay is $P_1 = (1 - K_0)P_T$. Assuming that $E\{a(n)a^*(m)\} = \delta(n - m)$, we can calculate α_{R_i} as (proof is skipped for brevity)

$$\alpha_{\mathrm{R}_i} = \begin{cases} \frac{1}{G_{\mathrm{SR}_i}P_0\left(1+\frac{1}{N}\sum_{k=1}^{2N-1}(2N-k)\left[g_{\mathrm{RC}}\left(\frac{kT_S}{2}\right)\right]^2\right)+2N_0} & \text{for FS-FDE} \\ \frac{1}{G_{\mathrm{SR}_i}P_0\left(1-\frac{\beta}{4}\right)+N_0} & \text{for SS-FDE} \end{cases} \quad (9)$$

where $g_{\mathrm{RC}} = g(t) * g^*(-t)$ is the impulse response of a raised cosine filter with the roll-off factor β, and symbol rate $1/T_S$. From (9), it is observed that in SS-FDE systems and for the special case of $\beta = 0$, a_{R_i} is reduced to the well-known form of $\frac{1}{G_{\mathrm{SR}_i}P_0+N_0}$ which is known as "fixed relay gain" [13].

After passing through the $\mathrm{R}_i \to \mathrm{D}$ channel and the input filter of the destination, the received signal is sampled at a rate of μ/T_S. The resulted signal is given by

$$\mathbf{y}_{\mathrm{R}_i\mathrm{D}}(n) = \sqrt{\frac{\mu G_{\mathrm{R}_i\mathrm{D}}\alpha_{\mathrm{R}_i}P_1}{N}} \sum_{k=-N}^{N} \tilde{H}_{\mathrm{R}_i\mathrm{D}}(k)\tilde{y}_{\mathrm{SR}_i}(k)W_N^{-k\varepsilon_{d,1}}W_{\mu N}^{-kn}$$
$$+ \mathbf{v}_{\mathrm{R}_i\mathrm{D}}(n) \quad (10)$$

for $n = 0, \ldots, \mu N - 1$, where $\tilde{H}_{\mathrm{R}_i\mathrm{D}}(k) = \tilde{h}_{\mathrm{R}_i\mathrm{D}}(k)\tilde{g}(k)\tilde{p}(k)$, $\tilde{h}_{\mathrm{R}_i\mathrm{D}}(k) \triangleq \tilde{h}_{\mathrm{R}_i\mathrm{D}}(\frac{k}{NT_S})$, $\tilde{h}_{\mathrm{R}_i\mathrm{D}}(f)$ is the continuous Fourier transform of $h_{\mathrm{R}_i\mathrm{D}}(t)$, $\tilde{y}_{\mathrm{SR}_i}(k) = \frac{1}{\sqrt{\mu N}}\sum_{n=0}^{\mu N-1}\mathbf{y}_{\mathrm{SR}_i}(n)W_{\mu N}^{kn}$, $\mathbf{v}_{\mathrm{R}_i\mathrm{D}}(n) = v_{\mathrm{R}_i\mathrm{D}}(\frac{nT_S}{\mu} + \varepsilon_{d,1}T_S)$, $v_{\mathrm{R}_i\mathrm{D}}(t)$ is a coloured complex Gaussian noise with $S_0(f) = N_0|\tilde{p}(f)|^2$, and $\varepsilon_{d,1}T_S$ is the sampling phase error in the destination during the relaying phase ($-N_{sp,2} \le \varepsilon_{d,1} \le 0$).

III. Equalization in the Frequency Domain

In the system under our consideration, after one broadcasting-relaying cycle, the destination has two received vectors $\mathbf{y}_{\mathrm{SD}}$, and $\mathbf{y}_{\mathrm{R}_i\mathrm{D}}$ (of size $\mu N \times 1$) given respectively by (6) and (10). After taking μN-point DFT of these signals, we have the following cases for the FS-FDE and SS-FDE systems.

Case 1: FS-FDE

In this case we have $\mu = 2$, $\tilde{p}(k) = \frac{1}{\sqrt{2}}$, and $S_0(f) = \frac{1}{2}N_0T_S\Pi(T_Sf/2)$ where $\Pi(f)$ is 1 for $-\frac{1}{2} \le f \le \frac{1}{2}$ and 0, otherwise. Therefore, based on (6), (7), and (10), we can write:

$$\tilde{\mathbf{y}}_{FSE,\mathrm{SD}} = \mathbf{Q}_{2N}\mathbf{y}_{\mathrm{SD}}|_{\mu=2} = \mathbf{D}_{FSE}\tilde{\mathbf{a}}_{2N} + \tilde{\mathbf{v}}_{FSE,\mathrm{SD}} \quad (11)$$

$$\tilde{\mathbf{y}}_{FSE,\mathrm{R}_i\mathrm{D}} = \mathbf{Q}_{2N}\mathbf{y}_{\mathrm{R}_i\mathrm{D}}|_{\mu=2} = \mathbf{D}_{FSE,i}\tilde{\mathbf{a}}_{2N} + \tilde{\mathbf{v}}_{FSE,\mathrm{R}_i\mathrm{D}}$$
$$+ \mathbf{C}_{FSE,i}\tilde{\mathbf{v}}_{FSE,\mathrm{SR}_i} \quad (12)$$

where $\tilde{\mathbf{a}}_{2N} = [\tilde{\mathbf{a}}^T|\tilde{\mathbf{a}}^T]^T$, $\tilde{\mathbf{a}} = \mathbf{Q}_N\mathbf{a}$, $\mathbf{D}_{FSE} = \mathrm{diag}\{\mathbf{d}_{FSE}\}$, $\mathbf{D}_{FSE,i} = \mathrm{diag}\{\mathbf{d}_{FSE,i}\}$, $\mathbf{C}_{FSE,i} = \mathrm{diag}\{\mathbf{c}_{FSE,i}\}$, $\mathbf{d}_{FSE}(k) = \sqrt{P_0}\tilde{h}_{\mathrm{SD}}([k]_N)\tilde{g}([k]_N)W_N^{-[k]_N\varepsilon_{d,0}}$, $\mathbf{d}_{FSE,i}(k) = \sqrt{2G_{\mathrm{R}_i\mathrm{D}}\alpha_{\mathrm{R}_i}P_1G_{\mathrm{SR}_i}P_0}\tilde{h}_{\mathrm{R}_i\mathrm{D}}([k]_N)(\tilde{g}([k]_N))^2\tilde{h}_{\mathrm{SR}_i}([k]_N) \times W_N^{-[k]_N(\varepsilon_{d,1}+\varepsilon_i)}$, $\mathbf{c}_{FSE,i}(k) = \sqrt{2G_{\mathrm{R}_i\mathrm{D}}\alpha_{\mathrm{R}_i}P_1}\tilde{h}_{\mathrm{R}_i\mathrm{D}}([k]_N) \times\tilde{g}([k]_N)W_N^{-[k]_N\varepsilon_{d,1}}$, $k = 0, \ldots, 2N - 1$. In (11) and (12), $\tilde{\mathbf{v}}_{FSE,\mathrm{SD}}$, $\tilde{\mathbf{v}}_{FSE,\mathrm{SR}_i}$, and $\tilde{\mathbf{v}}_{FSE,\mathrm{R}_i\mathrm{D}}$ are, respectively, the $2N$-point DFT of $\mathbf{v}_{\mathrm{SD}}$, $\mathbf{v}_{\mathrm{SR}_i}$ and $\mathbf{v}_{\mathrm{R}_i\mathrm{D}}$.

Case 2: SS-FDE

In this case we have μ=1, $\tilde{p}(k)$=$\tilde{g}^*(k)$, and $S_0(f)$=$N_0|\tilde{g}(f)|^2$. Therefore, based on (6), (7), and (10), we can write

$$\tilde{\mathbf{y}}_{SSE,\mathrm{SD}} = \mathbf{Q}_N\mathbf{y}_{\mathrm{SD}}|_{\mu=1} = \mathbf{D}_{SSE}\tilde{\mathbf{a}} + \tilde{\mathbf{v}}_{SSE,\mathrm{SD}} \quad (13)$$

$$\tilde{\mathbf{y}}_{SSE,\mathrm{R}_i\mathrm{D}} = \mathbf{Q}_N\mathbf{y}_{\mathrm{R}_i\mathrm{D}}|_{\mu=1} = \mathbf{D}_{SSE,i}\mathbf{C}_{SSE,i}\tilde{\mathbf{a}} + \tilde{\mathbf{v}}_{SSE,\mathrm{R}_i\mathrm{D}}$$
$$+ \mathbf{C}_{SSE,i}\tilde{\mathbf{v}}_{SSE,\mathrm{SR}_i} \quad (14)$$

where $\mathbf{D}_{SSE} = \mathrm{diag}\{\mathbf{d}_{SSE}\}$, $\mathbf{D}_{SSE,i} = \mathrm{diag}\{\mathbf{d}_{SSE,i}\}$, $\mathbf{C}_{SSE,i} = \mathrm{diag}\{\mathbf{c}_{SSE,i}\}$, $\mathbf{d}_{SSE}(k) = \sqrt{P_0}\sum_{m=k,k-N}\tilde{h}_{\mathrm{SD}}(m)|\tilde{g}(m)|^2W_N^{-m\varepsilon_{d,0}}$, $\mathbf{d}_{SSE,i}(k) = \sqrt{G_{\mathrm{SR}_i}P_0}\sum_{m=k,k-N}\tilde{h}_{\mathrm{SR}_i}(m)|\tilde{g}(m)|^2W_N^{-m\varepsilon_i}$, $\mathbf{c}_{SSE,i}(k) = \sqrt{G_{\mathrm{R}_i\mathrm{D}}\alpha_{\mathrm{R}_i}P_1}\sum_{m=k,k-N}\tilde{h}_{\mathrm{R}_i\mathrm{D}}(m)|\tilde{g}(m)|^2W_N^{-m\varepsilon_{d,1}}$. In (13) and (14), $\tilde{\mathbf{v}}_{SSE,\mathrm{SD}}$, $\tilde{\mathbf{v}}_{SSE,\mathrm{SR}_i}$, and $\tilde{\mathbf{v}}_{SSE,\mathrm{R}_i\mathrm{D}}$ are the N-point DFT of $\mathbf{v}_{\mathrm{SD}}$, $\mathbf{v}_{\mathrm{SR}_i}$ and $\mathbf{v}_{\mathrm{R}_i\mathrm{D}}$, respectively.

For both FS-FDE and SS-FDE cases, by concatenating the received signals in the frequency-domain into one column vector, we can write

$$\tilde{\mathbf{y}}_i = \mathbf{D}_i\tilde{\mathbf{A}} + \tilde{\mathbf{v}}_i. \quad (15)$$

For the case of FS-FDE, we have $\tilde{\mathbf{y}}_i = [\tilde{\mathbf{y}}_{FSE,\mathrm{SD}}^T|\tilde{\mathbf{y}}_{FSE,\mathrm{R}_i\mathrm{D}}^T]^T$, $\mathbf{D}_i = [\mathbf{D}_{FSE}|\mathbf{D}_{FSE,i}]^T$, $\tilde{\mathbf{A}} = [\tilde{\mathbf{a}}_{2N}^T|\tilde{\mathbf{a}}_{2N}^T]^T$, and $\tilde{\mathbf{v}}_i = [\tilde{\mathbf{v}}_{FSE,\mathrm{SD}}^T|(\mathbf{C}_{FSE,i}\tilde{\mathbf{v}}_{FSE,\mathrm{SR}_i} + \tilde{\mathbf{v}}_{FSE,\mathrm{R}_i\mathrm{D}})^T]^T$. On the other hand, for the case of SS-FDE, we have $\tilde{\mathbf{y}}_i = [\tilde{\mathbf{y}}_{SSE,\mathrm{SD}}^T|\tilde{\mathbf{y}}_{SSE,\mathrm{R}_i\mathrm{D}}^T]^T$, $\mathbf{D}_i = [\mathbf{D}_{SSE}|\mathbf{D}_{SSE,i}\mathbf{C}_{SSE,i}]^T$, $\tilde{\mathbf{A}} = \tilde{\mathbf{a}}_{2N} = [\tilde{\mathbf{a}}^T|\tilde{\mathbf{a}}^T]^T$, and $\tilde{\mathbf{v}}_i = [\tilde{\mathbf{v}}_{SSE,\mathrm{SD}}^T|(\mathbf{C}_{SSE,i}\tilde{\mathbf{v}}_{SSE,\mathrm{SR}_i} + \tilde{\mathbf{v}}_{SSE,\mathrm{R}_i\mathrm{D}})^T]^T$.

In the following, we derive the linear and decision feedback FDEs for both SS-FDE and FS-FDE scenarios.

A. Linear Equalization (LE)

The structure of the LE is depicted in Fig. 3a. The objective of the linear MMSE equalization is to find a weighting matrix, $\mathbf{M}_{LE,i}$, such that $E[\|\tilde{\mathbf{x}}_i - \tilde{\mathbf{a}}\|^2] = E[\|\mathbf{x}_i - \mathbf{a}\|^2]$ is minimized where $\tilde{\mathbf{x}}_i = \mathbf{M}_{LE,i}\tilde{\mathbf{y}}_i$ and $\mathbf{x}_i = \mathbf{Q}_{\mu N}^*\tilde{\mathbf{x}}_i$. Therefore, based on the so-called orthogonality principal, we have

$$E[(\tilde{\mathbf{x}} - \tilde{\mathbf{a}})\tilde{\mathbf{y}}^*] = \mathbf{0} \quad (16)$$

where we have dropped the sub-index i for the convenience. As a result, the weighting matrix is given by

$$\mathbf{M}_{LE} = (\mathbf{I} + \mathbf{J}\mathbf{D}^*\mathbf{\Gamma}_{\tilde{\mathbf{v}}}^{-1}\mathbf{D}\mathbf{J}^*)^{-1}\mathbf{J}\mathbf{D}^*\mathbf{\Gamma}_{\tilde{\mathbf{v}}}^{-1} \quad (17)$$

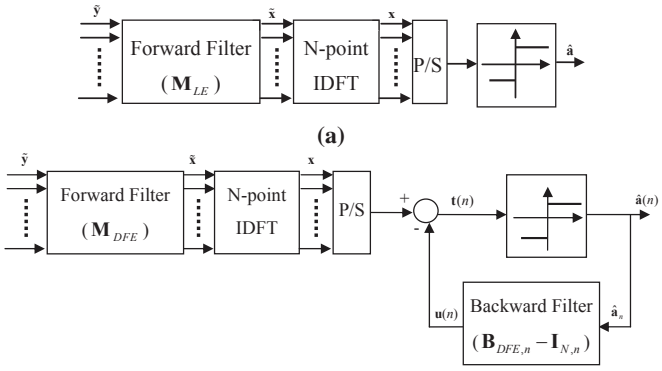

Fig. 3: Internal structure of the (a) FD-LE and (b) FD-DFE equalizers

where $\mathbf{J} = \mathbf{1}_{1\times 2\mu} \otimes \mathbf{I}_N$, and $\mathbf{\Gamma}_{\tilde{\mathbf{v}}} = N_0[\mathbf{I}_{2N}|\mathbf{C}_{FSE}\mathbf{C}^*_{FSE} + \mathbf{I}_{2N}]^T$ for the FS-FDE and $\mathbf{\Gamma}_{\tilde{\mathbf{v}}} = N_0[\mathbf{I}_N|\mathbf{C}_{SSE}\mathbf{C}^*_{SSE} + \mathbf{I}_N]^T$ for the SS-FDE. An N-point inverse DFT (IDFT) is applied to $\tilde{\mathbf{x}} = \mathbf{M}_{LE}\mathbf{y}$ and the resulting vector $\mathbf{x}$ is fed to a slicer device, operating on a symbol-by-symbol basis, to make a hard estimation about the transmitted vector $\mathbf{a}$. Defining the error autocorrelation matrix as $\mathbf{R}_e = \frac{1}{N}E[(\mathbf{x}-\mathbf{a})(\mathbf{x}-\mathbf{a})^*]$, by using (16) and (17) we can write

$$\mathbf{R}_e = \frac{1}{N}\mathbf{Q}^*(\mathbf{I}_N + \mathbf{J}\mathbf{D}^*\mathbf{\Gamma}^{-1}_{\tilde{\mathbf{v}}}\mathbf{D}\mathbf{J}^*)^{-1}\mathbf{Q} \tag{18}$$

Therefore, the associated MSE of the LE method is given by

$$MSE_{LE} = \mathrm{trace}(\mathbf{R}_e) = \frac{1}{N}\mathrm{trace}\left((\mathbf{I}_N + \mathbf{J}\mathbf{D}^*\mathbf{\Gamma}^{-1}_{\tilde{\mathbf{v}}}\mathbf{D}\mathbf{J}^*)^{-1}\right) \tag{19}$$

B. Decision-Feedback Equalization

The structure of the DFE is depicted in Fig. 3b. Similar to the LE, the received signal is first applied to a frequency-domain feed-forward filter, and then, returned back to the time domain via an IDFT operation to feed a symbol-by-symbol (hard-decision) slicer. However, in contrast to the LE, each detected symbol lines up in the input port of a feedback filter to contribute in the ISI reduction over the symbols that have not yet been detected. The output of the feedback filter at time instance n, $\mathbf{u}(n)$, can be considered as an estimation made based on $\hat{\mathbf{a}}(0),\ldots,\hat{\mathbf{a}}(n-1)$ about the ISI generated by the first $(n-1)$ transmitted symbols on the nth one. This output is then subtracted from $\mathbf{x}(n)$, and the resulting signal, i.e. $\mathbf{t}(n) = \mathbf{x}(n) - \mathbf{u}(n)$, is passed through the slicer where a hard estimation about the transmitted symbol $\mathbf{a}(n)$ is made. Feedback processing is carried out in the time domain through a time-varying finite-impulse response (FIR) filter. Considering an $N\times N$ unit lower triangular matrix $\mathbf{B}_{DFE}$, the output of the filter at time instance n, $\mathbf{u}(n)$, can be modelled as $\mathbf{u}(n) = (\mathbf{B}_{DFE,n} - \mathbf{I}_{N,n})\hat{\mathbf{a}}_n$ where $\mathbf{B}_{DFE,n}$ is the nth row of the matrix $\mathbf{B}_{DFE}$, $\mathbf{I}_{N,n}$ is the nth row of the matrix $\mathbf{I}_N$, and $\hat{\mathbf{a}}_n = [\hat{\mathbf{a}}(0),\ldots,\hat{\mathbf{a}}(n-1),\mathbf{0}_{1\times(N-n)}]^T$.

A performance measure of the DFE receiver is the error at the input of the decision device, i.e. $\mathbf{e} = \mathbf{t} - \mathbf{a}$. In the MMSE based DFE, the feedforward matrix $\mathbf{M}_{DFE}$ and the feedback matrix $\mathbf{B}_{DFE}$ are designed to minimize $E\|\mathbf{e}\|^2$. Using the standard assumption of correct past decisions, we have $\|\mathbf{e}\|^2 = \|\mathbf{t}-\mathbf{a}\|^2 = \|\tilde{\mathbf{x}} - \mathbf{Q}_N\mathbf{B}_{DFE}\mathbf{a}\|^2$.

Following the same approach in [14], we first assume that $\mathbf{B}_{DFE}$ is fixed. Accordingly, by using the orthogonality principle, $\mathbf{M}_{DFE}$ is given by

$$\mathbf{M}_{DFE} = \mathbf{Q}\mathbf{B}_{DFE}\mathbf{Q}^*(\mathbf{I} + \mathbf{J}\mathbf{D}^*\mathbf{\Gamma}^{-1}_{\tilde{\mathbf{v}}}\mathbf{D}\mathbf{J}^*)^{-1}\mathbf{J}\mathbf{D}^*\mathbf{\Gamma}^{-1}_{\tilde{\mathbf{v}}} \tag{20}$$

By defining $\mathbf{R}_e = \frac{1}{N}E[(\mathbf{t}-\mathbf{a})(\mathbf{t}-\mathbf{a})^*]$, then we can write

$$\mathbf{R}_e = \frac{1}{N}\mathbf{B}_{DFE}\mathbf{Q}^*(\mathbf{I} + \mathbf{J}\mathbf{D}^*\mathbf{\Gamma}^{-1}_{\tilde{\mathbf{v}}}\mathbf{D}\mathbf{J}^*)^{-1}\mathbf{Q}\mathbf{B}^*_{DFE} \tag{21}$$

Using the results in [14], $\mathrm{trace}(\mathbf{R}_e)$ is minimized by setting $\mathbf{B}_{DFE} = \mathbf{U}^{-1}$, where $\mathbf{U}$ is a unit lower triangular matrix given by the Cholesky decomposition of $\mathbf{Q}^*(\mathbf{I} + \mathbf{J}\mathbf{D}^*\mathbf{\Gamma}^{-1}_{\tilde{\mathbf{v}}}\mathbf{D}\mathbf{J}^*)^{-1}\mathbf{Q}$ in the form of $\mathbf{U}\mathbf{\Delta}\mathbf{U}^*$ where $\mathbf{\Delta}$ is a diagonal matrix with positive diagonal elements. Therefore, the MSE associated to the DFE is given by

$$MSE_{DFE} = \mathrm{trace}(\mathbf{R}_e) = \frac{1}{N}\mathrm{trace}(\mathbf{\Delta}) \tag{22}$$

Based on the MSE expressions derived in (19) and (22), we have the following proposition about the performance of the cooperative FS-FDE/SS-FDE equalization techniques under consideration.

Preposition: The performance of FS-FDE based cooperative equalizers does not depend on the sampling-phase error. On the other hand, for the case of SS-FDE based cooperative equalization, sampling-phase errors affect the system performance.

Proof: The proof is skipped for brevity.

The dependency of the FS-FDE method to sampling-phase errors is due to the superposition of the aliasing roll-off components. This superposition, for certain clock phases, may result in a spectral null, and subsequently, in the degradation of the SS-FDE performance [4, 5]. In the simulation results provided in the next section, we will demonstrate that this dependency significantly degrades the performance of the SS-FDE equalizers.

IV. Numerical Results

In this section, we investigate the bit error rate (BER) performance of cooperative systems with different equalization techniques based on Monte Carlo simulations. It is assumed that the selection of relays is based on maximizing the SNR at destination from the matched filter bound (MFB) persepective[2], $T_S = 1/2400$ sec, $\beta = 0.5$, and the adopted modulation scheme is BPSK and QPSK for the non-cooperative (i.e., direct transmission) and cooperative systems, respectively. Also, the bit SNR is denoted by E_b/N_0 where E_b is the energy per information bit.

Fig. 4 shows the BER performance of the SS-FDE- and FS-FDE- based linear equalization systems for $E_b/N_0 = 20$ dB, $G_{\mathrm{SR}_m} = 0$ dB, $G_{\mathrm{R}_m\mathrm{D}} = 0$ dB, $L_{\mathrm{SD}} = L_{\mathrm{SR}_m} = L_{\mathrm{R}_m\mathrm{D}} = 2$, and equal power allocation ($K_0 = 0.5$). We assume various sampling-phase errors at the relay(s) and destination terminals when the delay spread is $5T_S$. It is observed from these results that the performance of SS-FDE-based systems is highly dependent on the variations of the sampling-phase error. In particular, for certain values of errors, the BER performances of the cooperative schemes approach to that of no-relay system whereas FS-FDE successfully compensates the phasing-error and retains the cooperative diversity.

Fig. 5 displays the BER performance of FS-FDE- and SS-FDE- based linear equalization for systems with different number of relays. We assume $G_{\mathrm{SR}_m} = 0$ dB, $G_{\mathrm{R}_m\mathrm{D}} = 10$ dB, $L_{\mathrm{SD}} = L_{\mathrm{SR}_m} = L_{\mathrm{R}_m\mathrm{D}} = 2$, and the delay spread is $5T_S$. By solving the optimum (from MFB perspective) power allocation problem [15], the value of K_0 is found to be 0.77 and 0.67 for the one- and two-relay cooperative systems under consideration, respectively. The sampling phase error

[2]From MFB perspective, in a multi-relay opportunistic cooperative system, the optimum relay selection rule is given by $i = \arg\max_m \frac{G_{\mathrm{SR}_m}G_{\mathrm{R}_m\mathrm{D}}\|\mathbf{h}_{\mathrm{SR}_m}\|^2\|\mathbf{h}_{\mathrm{R}_m\mathrm{D}}\|^2}{\bar{\gamma}^{-1}+K_0+G_{\mathrm{R}_m\mathrm{D}}\|\mathbf{h}_{\mathrm{R}_m\mathrm{D}}\|^2(1-K_0)}$ where $\bar{\gamma} = P_T/N_0$ [15].

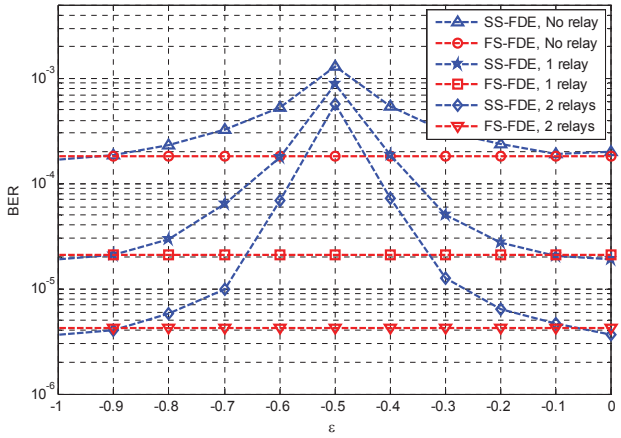

Fig. 4: BER performances of SS-FDE and FS-FDE systems with different number of relays with respect to different sampling phase errors.

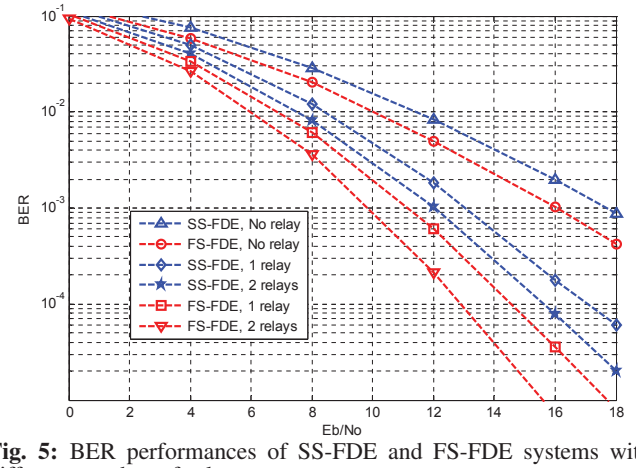

Fig. 5: BER performances of SS-FDE and FS-FDE systems with different number of relays.

at the relay(s) and destination terminals is randomly chosen with uniform distribution from the interval $[-T_S, 0]$ for each transmitted block. It is observed from Fig. 5 that the FS-FDE method outperforms the SS-FDE approach. Specifically, at a target BER of 10^{-3}, the performance gap between the FS-FDE- and SS-FDE-based methods is 1.6 dB for the non-cooperative scenario. This performance gap climbs up to 1.9 and 2.25 dB for cooperative systems with one and two relays, respectively.

Fig. 6 shows the BER performance of DFE- and LE-techniques for both SS-FDE- and FS-FDE-based one-relay cooperative systems under the uniform random sampling phase errors. We assume that $G_{\mathrm{SR}_1} = 0$ dB, $G_{\mathrm{R}_1\mathrm{D}} = 10$ dB, $L_{\mathrm{SD}} = L_{\mathrm{SR}_1} = 5$, $L_{\mathrm{R}_1\mathrm{D}} = 10$, and the delay between consecutive paths is T_S. For this case, based on the MFB analysis, the optimum value of K_0 is 0.82 [15]. It is observed that the DFE methods outperform the corresponding LE approaches. Specifically, at a target BER of 10^{-4}, the performance gap between the DFE- and LE-methods are 1.6 and 3 dB for the SS-FDE- and FS-FDE-based systems, respectively. Moreover, based on Fig. 6, FS-FDE-systems (with either LE or DFE technique) outperform the SS-FDE-systems in exploiting the available multipath diversity in the underlying channels.

V. Conclusion

In this paper, we have investigated FS-FDE for a cooperative multi-relay system. Specifically, we have proposed a $T_S/2$-spaced equalizer that transforms the temporal sample sequence to the frequency domain, applies either linear or decision-feedback equalization, and returns the resulting signal back to the time domain for detection. We have demonstrated that, under specific channel realizations and sampling

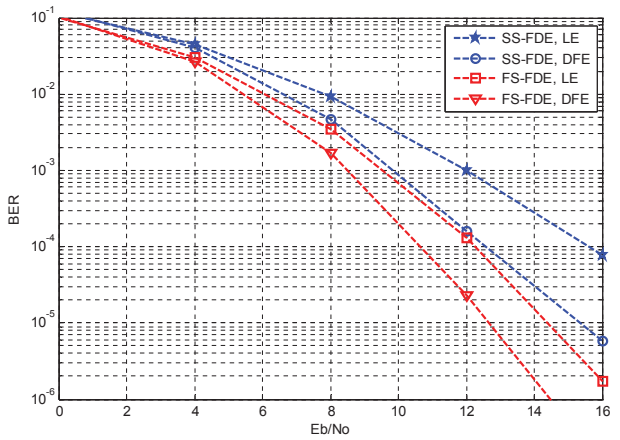

Fig. 6: BER performances of single-relay assisted SS-FDE and FS-FDE systems with LE and DFE equalizations.

errors, the cooperative systems with SS-FDE fail to harvest the available cooperative diversity and its BER performance gap is degraded by 1 and 2 orders of magnitudes (with respect to the proposed FS-FDE method) when using one and two relays, respectively.

References

[1] J. Laneman, D. Tse, and G. Wornell, "Cooperative diversity in wireless networks: Efficient protocols and outage behavior," *IEEE Trans. Inf. Theory*, vol. 50, no. 12, pp. 3062 – 3080, Dec. 2004.

[2] E. Biglieri, J. Proakis, and S. Shamai, "Fading channels: information-theoretic and communications aspects," *IEEE Trans. Inf. Theory*, vol. 44, no. 6, pp. 2619 –2692, Oct. 1998.

[3] S. Qureshi, "Adaptive equalization," *Proceedings of the IEEE*, vol. 73, no. 9, pp. 1349 – 1387, Sep. 1985.

[4] R. D. Gitlin and S. B. Weinstein, "Fractionally-spaced equalization: An improved digital transversal equalizer," *Bell Syst. Tech. J.*, vol. 60, p. 275296, Feb. 1981.

[5] G. Ungerboeck, "Fractional tap-spacing equalizer and consequences for clock recovery in data modems," *IEEE Trans. Commun.*, vol. 24, no. 8, pp. 856 – 864, Aug. 1976.

[6] F. Pancaldi and G. Vitetta, "Block channel equalization in the frequency domain," *IEEE Trans. Commun.*, vol. 53, no. 3, pp. 463 – 471, Mar. 2005.

[7] M. Clark, "Adaptive frequency-domain equalization and diversity combining for broadband wireless communications," *IEEE J. Sel. Areas Commun.*, vol. 16, no. 8, pp. 1385 –1395, Oct. 1998.

[8] R. Kalbasi, D. Falconer, A. Banihashemi, and R. Dinis, "A comparison of frequency-domain block MIMO transmission systems," *IEEE Trans. Veh. Technol.*, vol. 58, no. 1, pp. 165 –175, Jan. 2009.

[9] H. Mheidat, M. Uysal, and N. Al-Dhahir, "Equalization techniques for distributed space-time block codes with amplify-and-forward relaying," *IEEE Trans. Signal Process.*, vol. 55, no. 5, pp. 1839 –1852, May 2007.

[10] H. Chen, A. Gershman, and S. Shahbazpanahi, "Filter-and-forward distributed beamforming in relay networks with frequency selective fading," *IEEE Trans. Signal Process.*, vol. 58, no. 3, pp. 1251 –1262, Mar. 2010.

[11] Y.-w. Liang, A. Ikhlef, W. Gerstacker, and R. Schober, "Cooperative filter-and-forward beamforming for frequency-selective channels with equalization," *IEEE Trans. Wireless Commun.*, vol. 10, no. 1, pp. 228 –239, Jan. 2011.

[12] P. Wu and R. Schober, "Cooperative frequency-domain beamforming for broadband SC-FDE systems," in *Proceedings of IEEE GLOBECOM*, Dec. 2011, pp. 1 –6.

[13] M. Hasna and M.-S. Alouini, "A performance study of dual-hop transmissions with fixed gain relays," *IEEE Trans. Wireless Commun.*, vol. 3, no. 6, pp. 1963 – 1968, Nov. 2004.

[14] A. Stamoulis, G. Giannakis, and A. Scaglione, "Block FIR decision-feedback equalizers for filterbank precoded transmissions with blind channel estimation capabilities," *IEEE Trans. Commun.*, vol. 49, no. 1, pp. 69 –83, Jan. 2001.

[15] M. R. Heidarpour, *Cooperative Techniques for Next Generation HF Communication Systems*. PhD thesis, University of Waterloo, Mar. 2013.